

Novel catalysts for advanced hydroprocessing: transition metal phosphides

S. Ted Oyama

Environmental Catalysis and Materials Laboratory, Department of Chemical Engineering, Virginia Tech, Blacksburg, VA 24061, USA

Received 15 August 2002; revised 18 September 2002; accepted 23 September 2002

Abstract

The field of catalysis is continuously invigorated by the discovery of new catalytic materials. Transition metal phosphides represent one such group of compounds that have recently been shown to have excellent activity for hydrodesulfurization (HDS) and hydrodenitrogenation (HDN). This is an important area, as continuous decline in the quality of petroleum feedstocks and increasingly stringent environmental regulations have made the removal of sulfur a paramount problem in the refining industry. The structure of the metal-rich phosphides is based on trigonal prisms, which can well accommodate the relatively large phosphorus atoms. The prisms are similar to those in sulfides, but phosphides do not take on layered structures and are metal conductors, not insulators or semiconductors. Lack of layers leads to a more isotropic crystal morphology and potentially better exposure of surface metal atoms to fluid phase reactants. Phosphides can be prepared readily in bulk and supported forms by reduction of phosphate precursors. The catalytic activity of the phosphides for dibenzothiophene HDS and quinoline HDN at 643 K and 3.1 MPa followed the order $\text{Fe}_2\text{P} < \text{CoP} < \text{MoP} < \text{WP} < \text{Ni}_2\text{P}$. The best catalyst, $\text{Ni}_2\text{P}/\text{SiO}_2$, had better activity in hydroprocessing than a commercial $\text{Ni-Mo-S}/\text{Al}_2\text{O}_3$ (HDS 98% vs 78% and HDN 80% vs 43%), based on equal sites loaded in the reactor. The sites were titrated by CO chemisorption at room temperature for the phosphides and by pulse O_2 chemisorption at dry-ice acetone temperatures for the sulfide. The $\text{Ni}_2\text{P}/\text{SiO}_2$ also compared favorably with a commercial $\text{Co-Mo-S}/\text{Al}_2\text{O}_3$ catalyst (Ketjenfine 756) using a real feed at 593 K and 3.9 MPa. On the basis of equal weights loaded in the reactor, the Ni_2P was again found to have higher performance than the sulfide (HDS 85% vs 80%). Studies of $\text{Ni}_2\text{P}/\text{SiO}_2$ catalysts with varying Ni/P ratios indicated that the principal phase remained Ni_2P , but that the crystallite size decreased with increasing P content as a result of facilitated contact on the surface between the Ni component and the phosphorus reagent. Activity measurements on these samples indicated that HDS was structure-insensitive, but that HDN was structure-sensitive. Extended X-ray absorption fine structure measurements indicated that the surface formed a phospho sulfide after reaction. The mechanism of HDN was investigated using a series of molecular probes of varying structure. The reactivity order for pentylamines indicated that C–NH₂ bond scission proceeded by a β -hydride elimination mechanism, similar to that occurring on sulfides. The reactivity order of substituted piperidines indicated that ring-opening proceeded by C–N bond scission and involved an α -carbon, and thus was different from the pathway on sulfides, which again appeared to involve a β -hydride elimination. This difference may account for the higher activity of phosphides over sulfides.

© 2003 Elsevier Science (USA). All rights reserved.

Keywords: Metal phosphides; EXAFS; MAS-NMR; Hydrodesulfurization; Hydrodenitrogenation

1. Introduction

New catalytic materials play an important role in the discovery and improvement of processes for the conversion of energy, the production of chemicals, and the elimination of pollutants. For example, the past 10 years have seen great advances in the areas of automotive emissions control, fine chemicals production, syngas conversion, and ox-

idative transformations, driven by the development of new catalysts [1,2].

One area which has witnessed considerable activity in the last decade is hydroprocessing. This has been the result of a global tightening in the allowed sulfur content in fuels and increased restrictions on the release of nitrogen oxides [3,4]. These trends have led to a worldwide search for better catalysts for hydrodesulfurization (HDS) and hydrodenitrogenation (HDN) [5]. Current approaches include the improvement of existing sulfide catalysts and the investigation of new compositions such as bimetallic carbides [6], ni-

E-mail address: oyama@vt.edu.

trides [7], and materials containing noble metals [8,9]. This account reports on a novel class of compounds that have substantial promise as next-generation catalysts. The materials are the transition metal phosphides, a group of stable, sulfur-resistant, metallic compounds that have exceptional hydroprocessing properties. Recent work has shown that MoP [10–14], WP [15,16], Ni₂P, and Co₂P [17–19] are highly active for HDS and HDN of petroleum feedstocks.

The strong suppression of sulfur removal by nitrogen compounds [20] is a fundamental problem which is exacerbated by the decline in the overall quality of crudes. Moreover, it is well recognized that HDN is more difficult than HDS, requiring more severe conditions of pressure and temperature. Thus, nitrogen removal is a key problem in HDS, in particular deep HDS to levels of 50 ppm S or less.

Since the phosphides are not well known in the field of catalysis, a brief introduction to their physical and structural properties and methods of preparation will be given. This will be followed by a review of their hydrotreating properties. Special emphasis will be placed on analyzing the mechanism of HDN, as this is a structure-sensitive reaction that can give insight on the site requirements on the surface of the catalysts. As will be seen, the most active of the phosphides, nickel phosphide (Ni₂P), provides a unique reaction pathway for nitrogen removal from organic molecules which involves activation at carbon positions α and β to nitrogen atoms. This is in contrast to sulfides, which carry out HDN principally through activation at the β position.

2. General properties

Phosphorus reacts with most elements of the periodic table to form a diverse class of compounds known as phosphides. The bonding in these materials ranges from ionic for the alkali and alkaline earth metals to metallic or covalent for the transition elements and covalent for the main group elements. The focus of this paper concerns the metal-rich compounds, MP or M₂P, of the transition metals, which have metallic properties. The phosphorus-rich compositions are semiconducting and are considerably less stable than the metal-rich compounds.

The nature, structure, and synthesis of phosphides have been described in a number of reviews [21,22]. Only the properties of the metal-rich phosphides will be considered here. Basically, these phosphides have physical properties similar to those of ordinary metallic compounds such as carbides, nitrides, borides, and silicides. Thus, they are good conductors of heat and electricity, are hard and strong, and have high thermal and chemical stability (Table 1).

Table 1
Physical properties of metal-rich phosphides

Melting points K	Heats of formation kJ mol ⁻¹	Microhardness kg mm ⁻²	Resistivity $\mu\Omega$ cm
> 1300	> 85	~ 600	< 200

Although the physical and chemical properties of phosphides resemble those of carbides and nitrides, they differ substantially in their crystal structure. In the carbides and nitrides, the carbon and nitrogen atoms reside in the interstitial spaces between metal host atoms to form relatively simple lattices: face-centered cubic, hexagonal close-packed, or simple hexagonal. For these compounds, geometric considerations predict stable structures when the ratio of nonmetal to metal radii (r_X/r_M) is between 0.41 and 0.59 [23]. For the phosphides, however, the atomic radius of phosphorus (0.109 nm) is substantially larger than that of carbon (0.071 nm) or nitrogen (0.065 nm) and the radius ratio is too large for octahedral coordination around the nonmetal to be favorable. For this reason, in phosphides (also borides and silicides), the nonmetal atom is usually found at the center of a triangular prism [21]. Different arrangements of these building blocks give rise to different structures.

3. Structure

A summary of the different crystal forms is given in Fig. 1 [24]. MoP is isostructural with WC, with the nonmetal-containing prisms stacked on top of each other. VP has the Ni–As structure with the P-prisms displaced laterally one-half lattice spacing. NbP and TaP adopt the closely related NbAs structure, which just differs from VP in the way the prisms are stacked. The monophosphides of groups 6–10 adopt the MnP and NiP structures both of which can be regarded as distortions of the NiAs structure. In the MnP

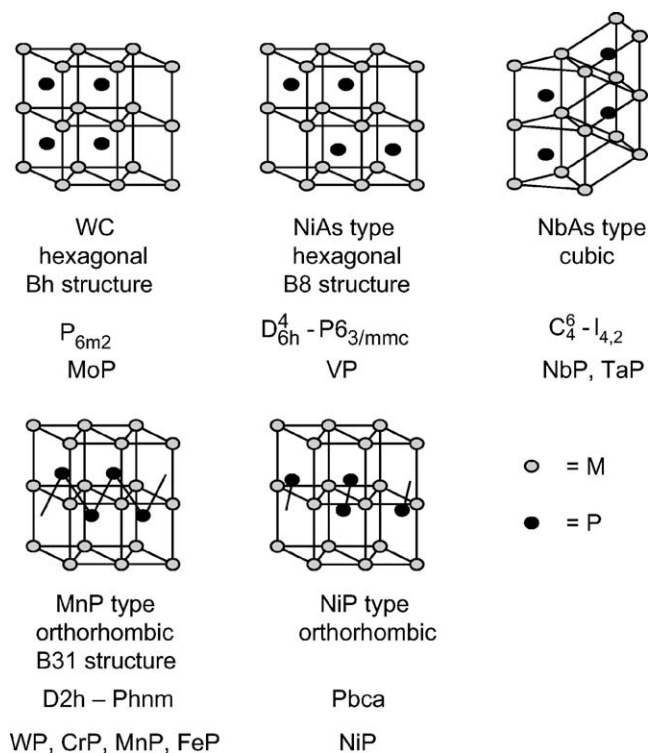


Fig. 1. Structure of transition metal phosphides.

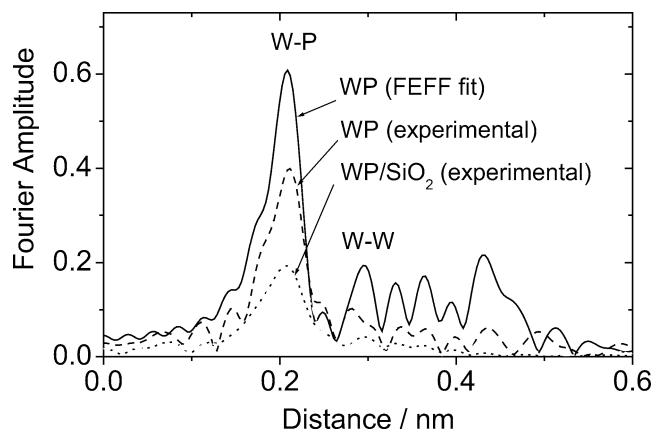


Fig. 2. Comparison of WL_3 -edge EXAFS spectra of WP and WP/SiO₂. (Reproduced from Ref. [16], with permission.)

structure the phosphorus atoms form chains, while in the NiP structure the phosphorus atoms form pairs.

The structure of the phosphides can be probed by extended X-ray absorption fine structure (EXAFS) measurements. WP is an example (Fig. 2). The data were taken in special cells without exposure of the samples to the atmosphere. The Fourier transformed spectra show characteristic distances for W–P and W–W bonds which are close in bulk and supported samples. A FEFF simulation gives excellent agreement with crystallographically reported distances [16].

Characterization of phosphides by ³¹P magic angle spinning nuclear magnetic resonance (MAS-NMR) spectroscopy yields additional information about the structure and bonding in the materials. WP again provides a good example (Fig. 3a) [13]. At zero rotation the bulk sample shows an asymmetric envelope, characteristic of considerable electric-field anisotropy surrounding the phosphorus nucleus. This can be understood from its crystal structure (Fig. 1), which shows that the phosphorus atoms reside in sites that look different when approached from the *x*, *y*, or *z* directions. When the sample is rotated, the anisotropy spills over to the spinning side bands, resulting in a complex intensity pattern.

Nevertheless, crystallographically all the P atoms are equivalent, and so the position of only one major peak in the sample (255 ppm referenced to 85% H₃PO₄) was invariant with spinning.

The NMR measurements are also important for characterizing well-dispersed, supported samples as well as identifying minority phases. Examination of the pattern for WP/SiO₂ (Fig. 3b) again shows the isotropic peak (255 ppm) due to WP, but in addition there is another substantial peak (–6 ppm), which is characteristic of a phosphate species. The phosphate probably represents a remnant of the starting material that was unreduced and is probably localized on the support. These measurements were carried out with the same samples as for the EXAFS determinations reported above, again without exposing the materials to the atmosphere. The EXAFS of the W-edge was unable to detect the presence of the phosphate, demonstrating how different techniques give different types of information.

The measured NMR shift for the phosphides is a Knight shift resulting from the interaction of P nuclei with the conduction electrons of the solid [16]. The shift differs in magnitude and sign from the chemical shifts of phosphate compounds and indicates the metallic nature of the phosphide. MAS-NMR has recently been employed to characterize other phosphides, including MoP with Knight shift of 214 ppm [13], Ni₃P with shift of 1796 ppm, and Ni₂P with shifts of 1487 and 4076 ppm [25]. MoP and Ni₃P give rise to one resonance and Ni₂P to two because of the presence of, respectively, one and two types of P atoms in the structures.

Both phosphides and sulfides adopt trigonal prisms as fundamental blocks in building up crystal structures. However, in sulfides a common trend is the adoption of layered structures, whereas in phosphides this is not the case. This has a considerable impact on the morphology of supported catalysts. Sulfides generally possess flat, two-dimensional crystal habits that expose saturated basal planes, while phosphides have more isotropic external morphologies that give rise to globular shapes. A nice example of this motif is shown (Fig. 4) for MoP/SiO₂ [13]. The consequence for catalytic

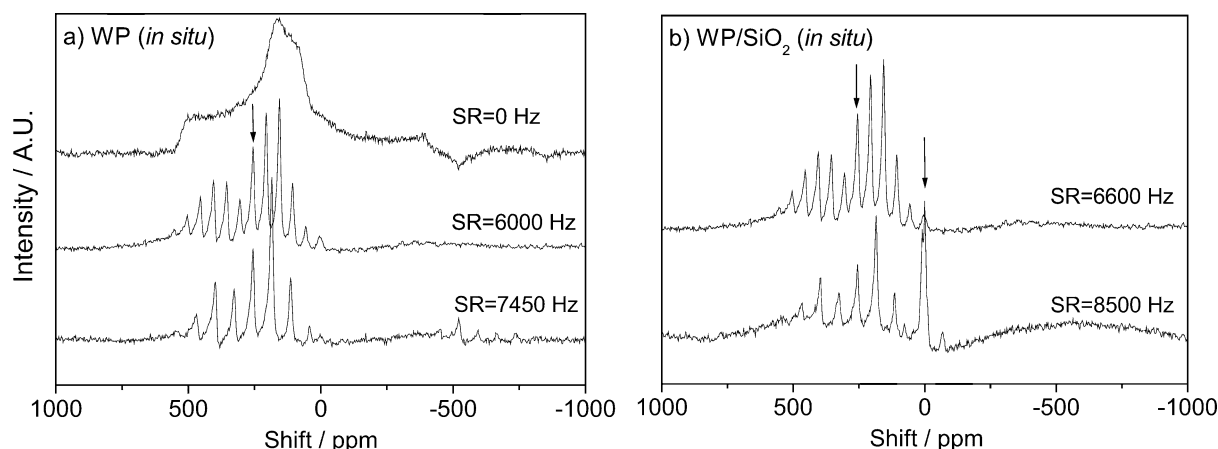


Fig. 3. Comparison of ³¹P MAS-NMR spectra of WP and WP/SiO₂. (Reproduced from Ref. [14], with permission.)

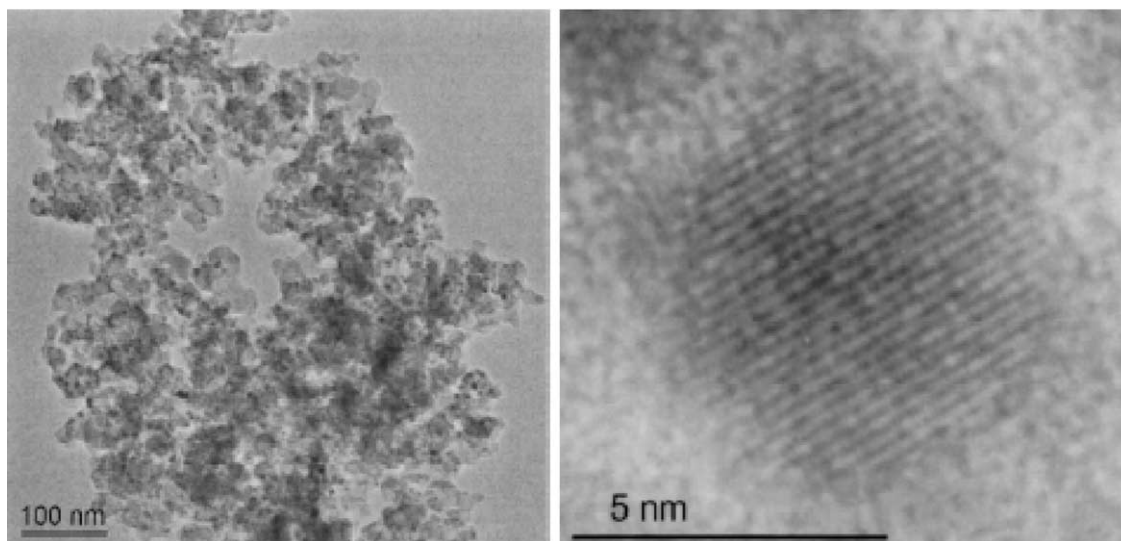


Fig. 4. Electron micrographs of MoP/SiO₂ catalysts. (Reproduced from Ref. [13], with permission.)

activity can be substantial, for phosphides potentially can expose a greater number of coordinatively unsaturated surface atoms, and hence give rise to higher site densities.

4. Synthesis

Numerous methods have been reported for the preparation of phosphides (Table 2). The most common is the synthesis from the elements, which can be carried out in different manners including ampoule techniques and arc melting. For catalysis applications many of these preparation methods are impractical because they require high temperatures, utilize expensive starting materials, or produce extraneous species which can contaminate the product. As will be shown, a convenient and simple method of synthesis is the reduction of phosphates, which can be carried out at moderate temperatures.

An example of a synthesis trace is given for WP (Fig. 5) [15]. The precursor was the phosphate, WPO₆, prepared from ammonium paratungstate and ammonium phosphate, and the heating rate was 0.0167 K s⁻¹ (1 °C min⁻¹). There is one main reduction feature at ~ 900 K, which is accompanied by an increase in surface area and chemisorption uptake of CO. The latter measurements were carried out with

Table 2
Synthesis of phosphides

Method	Reaction
Combination of the elements	$M^0 + xP^0(\text{red}) \rightarrow MP_x$
Solid state metathesis	$MCl_x + Na_3P \rightarrow MP + NaCl$
Reaction with phosphine	$MCl_x + PH_3 \rightarrow MP + HCl + H_2$
Decomposition of organometallics	$TiCl_4(PH_2C_6H_{11})_2 \rightarrow TiP + PH_3 + HCl + C_6H_{10}$
Electrolysis of fused salts	$MO_x + NaPO_y \rightarrow MP + Na_2O$
Reduction of phosphates	$MPO_x + H_2 \rightarrow MP + xH_2O$

different samples by interrupting the experiments at different stages in the reduction.

The material shows a modest surface area and CO uptake. These values and those of other phosphides are presented in Table 3. Because of these low values, the materials were also synthesized in supported form on SiO₂. Silica was chosen as a support in order to minimize support interactions, and high loadings (~ 12 wt%) were used in order to facilitate analysis of the products by X-ray diffraction. The synthesis traces for the supported samples were essentially identical to the unsupported references, and XRD duly showed the presence of the expected phosphides.

5. Catalytic properties

There have been relatively few studies of the catalytic behavior of phosphides. In general the phosphides catalyze the hydrogenation of alkenes, alkynes, dienes, and nitrocom-

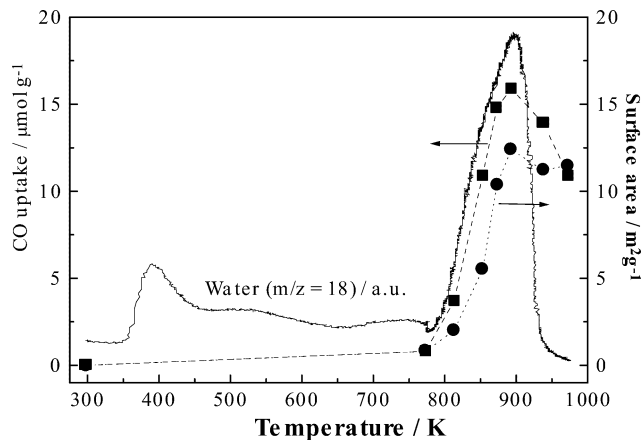


Fig. 5. Synthesis of WP by temperature-programmed reduction. (Reproduced from Ref. [15], with permission.)

Table 3
Surface area and CO chemisorption in SiO₂-supported and bulk phosphides

Catalyst	13 wt% MoP/SiO ₂ ^a	20 wt% WP/SiO ₂ ^a	14 wt% Fe ₂ P/SiO ₂ ^b	9 wt% CoP/SiO ₂ ^a	10 wt% Ni ₂ P/SiO ₂ ^a
SA ^c (m ² g ⁻¹)	50 (8)	62 (10)	97 (3)	87 (3)	97 (3)
CO uptake ^c (μmol g ⁻¹)	50 (15)	19 (10)	16 (3)	16 (3)	28 (4)

^a Metal loading = 1.16 mmol g⁻¹ SiO₂.

^b Metal loading = 2.31 mmol g⁻¹ SiO₂.

^c (Parenthesis) = bulk value.

pounds [26]. For the iron group metals the order of activity in 1-butene hydrogenation was [27] Ni₂P > Co₂P > FeP, with Ni₂P also having better selectivity for the partial hydrogenation of dienes [28]. Amorphous Ni–P alloys prepared by chemical reduction [29] or an electroless plating technique [30] have also been reported to be active for hydrogenation. Compared to Ni metal, Ni–P had slightly higher turnover rates [31,32].

Heats of adsorption of CO and H₂ have been measured calorimetrically on amorphous Ni phosphide [33]. Compared to Ni metal where the initial heats were respectively 120 and 85 kJ mol⁻¹, the heats on the phosphide were respectively 30 and 20 kJ mol⁻¹ lower. The decrease in the heats was attributed to electron withdrawal by the electronegative P atoms.

The first reports of the application of phosphides in HDN [17] and simultaneous HDS and HDN have appeared only recently [10]. In HDN it was found that Ni₂P had higher activity for quinoline denitrogenation than a commercial sulfided Ni–Mo/Al₂O₃ catalyst. Deviations in the kinetics of the reaction network suggested that the two systems worked in fundamentally different manners, that is, the activity of the Ni–Mo sulfide was not due to the formation of Ni₂P on its surface. In simultaneous HDN and HDS, MoP was found to have moderate activity compared to a commercial Ni–Mo/Al₂O₃ catalyst, but with better quinoline HDN. In a subsequent study of HDN of orthopropylamine, it was confirmed that MoP had six times higher activity per site than a sulfided Mo/Al₂O₃ catalyst [11]. Also, a supported 15 wt% MoP/SiO₂ catalyst was found to be nearly four times more active in the hydrodesulfurization of thiophene [13] than a sulfided Mo/SiO₂ catalyst.

The catalytic activity of a series of phosphides for HDN and HDS was compared (Fig. 6) in a trickle bed reactor operated under industrial conditions. The reactant feed was a model feed containing quinoline (2000 ppm N), dibenzothiophene (3000 ppm S), tetralin (20 wt%), and tetradecane (balance). An amount corresponding to 70 μmol of chemisorption sites (CO for the phosphides, O₂ for the sulfide) was loaded into the reactor.

The activity of the catalysts improved in the order Fe₂P < CoP < MoP < WP < Ni₂P. The results for tungsten phosphide and nickel phosphide are notable. In the difficult HDN reaction tungsten phosphide had higher conversion than the commercial Ni–Mo catalyst (58 vs 38%), while nickel phosphide had substantially higher activity in both

HDS (98 vs 77%) and HDN (90 vs 38%). The overall activity of the nickel phosphide was superior to that of the sulfide on a surface area (SA) basis (also turnover rate). These levels of activity were higher than those of the best bimetallic carbides and nitrides and were surprising, as the phosphide was a simple monometallic compound. Also very attractive was the fact that the phosphide showed lower hydrogenation activity than the sulfide, indicating a more effective use of hydrogen.

Results with model compounds often do not correlate with those obtained with real feeds because the interactions between the components are complex, so most catalyst development is carried out with actual feeds. In order to evaluate the potential of the Ni₂P/SiO₂ it was subjected to a test with a hydrotreated gas oil [34]. This feed was chosen because of its low sulfur (440 ppm) and nitrogen (8 ppm) content and moderate aromatics content (27 wt%), which mimics that which would be used in a second-stage hydrotreating process. The measurements were made again in a trickle-flow system, but comparison this time was made on an equal-weight basis with a current commercial Co–Mo–S/Al₂O₃ catalyst (Ketjenfine 756) of surface area 218 m² g⁻¹ and containing 11.2 wt% Mo and 3.1 wt% Co [35].

The Ni₂P/SiO₂ (initial P/Ni = 2/1) compared favorably with the Co–Mo–S/Al₂O₃ catalyst in HDS conversion (85 vs 80%) and exit sulfur content (66 vs 86 ppm) (Fig. 7). The comparison at the same weight hourly space velocity is

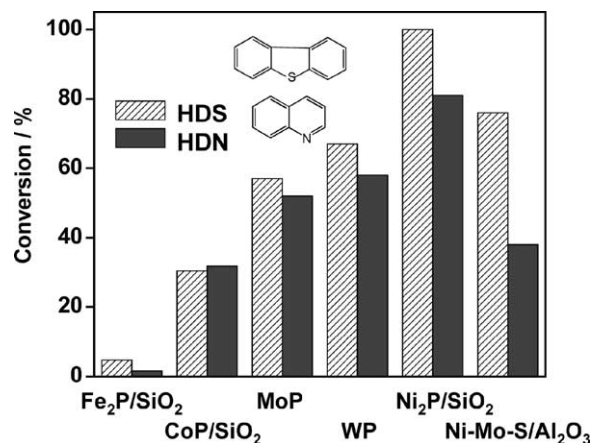


Fig. 6. Comparison of different phosphides in the hydroprocessing of a model feed. $T = 643$ K (370 °C) and $P = 3.1$ MPa (450 psig); liquid feed = 5 cm³ h⁻¹; gas flow = 150 cm³ (NTP) min⁻¹; bed volume = 1 cm³.

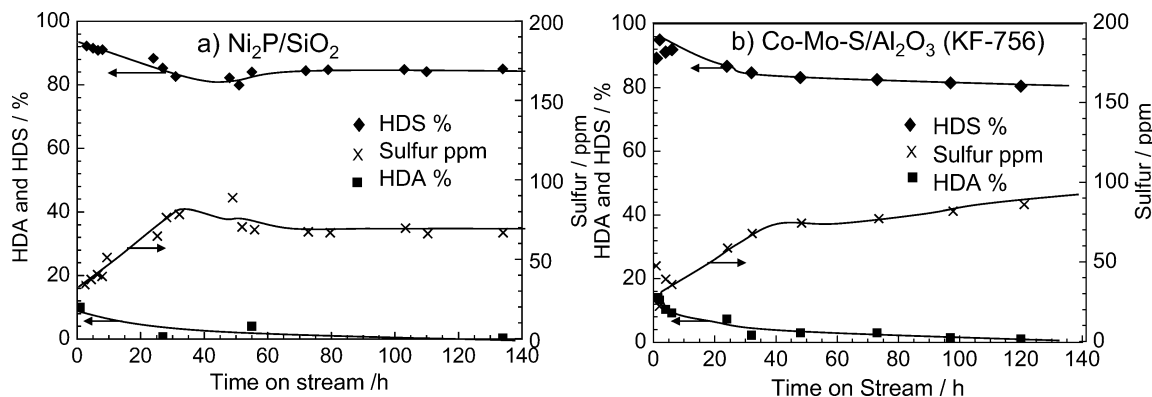


Fig. 7. Comparison of (a) $\text{Ni}_2\text{P}/\text{SiO}_2$ and (b) $\text{Co-Mo-S}/\text{Al}_2\text{O}_3$ in the hydroprocessing of a real feed. $T = 593 \text{ K}$ ($320 \text{ }^\circ\text{C}$) and $P = 3.9 \text{ MPa}$ (570 psig); liquid feed = 4.0 g h^{-1} , WHSV = 4 h^{-1} , amount of catalyst = 1 g. \blacklozenge = % HDS, \times = Exit sulfur ppm, \blacksquare = % HDA (hydrodearomatization). (Reproduced from Ref. [34], with permission.)

important for reactor sizing. A comparison based on surface area would be even more favorable to the $\text{Ni}_2\text{P}/\text{SiO}_2$, which used a low-surface-area ($90 \text{ m}^2 \text{ g}^{-1}$), low-density, fumed support. The phosphide catalyst showed significant superiority to the sulfide in two other respects. It had a lower HDA conversion (0.7 vs 1.1%). This is desirable in order to limit hydrogen consumption in the final stages of processing and to avoid disruption of the hydrocarbon structure, which can result in cracking. The phosphide also displayed a more rapid attainment of steady state and no deactivation. Overall, in terms of activity, selectivity, and stability, the phosphide was superior to the commercial catalyst. This is surprising, since the phosphide is an unpromoted, single-metal catalyst placed on a relatively unattractive support.

The effect of phosphorus content on the hydroprocessing performance of the supported $\text{Ni}_2\text{P}/\text{SiO}_2$ catalyst was studied [36] (Fig. 8). The catalyst composition is described using the initial P/Ni ratio employed in the synthesis, but actual P levels were lower due to loss of PH_3 during reduction of the catalysts. The P/Ni = 2/1 sample actually was close to stoichiometric Ni_2P . As can be seen, the HDS conversion did not change appreciably with initial P/Ni ratio, but the HDN conversion went through a maximum.

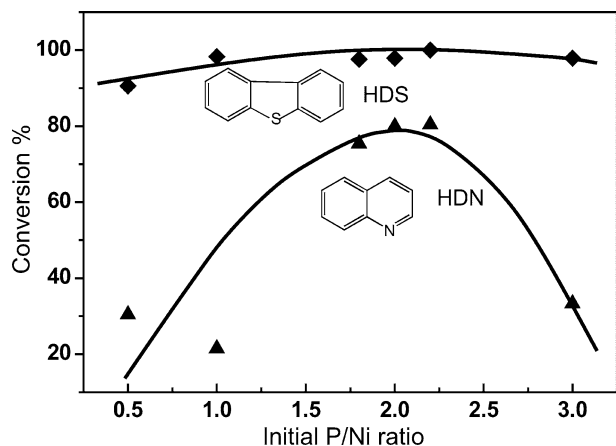
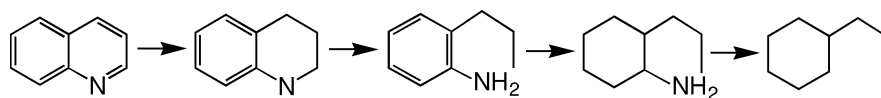


Fig. 8. Effect of composition on Ni_2P activity. (Reproduced from Ref. [36], with permission.)

The effect of P content on HDS and HDN on these samples gives insight into the nature of the active sites responsible for these reactions. It was found that the crystallite size of the materials decreased with increasing P content. This was probably due to better contact on the surface between the nickel component and the phosphorus reagent during the synthesis of the catalyst. But the size range of the crystallites was small, 7–26 nm, so a classical particle size effect is unlikely. Rather, the effect on reactivity is likely due to changes in the composition of the supported crystallites. In the case of HDS the small effect of P content on conversion suggests that the reaction occurs principally on metal centers and that there is little effect of ensemble size on reactivity. Hence, the reaction is structure-insensitive. The reaction may occur by direct sulfur removal from dibenzothiophene, as no hydrogenated intermediates were observed [36].

In contrast, in the case of HDN, the relatively large effect of P on conversion suggests that P affects the catalytic center indirectly, by altering its structure, or directly, by being part of the active site. The HDN of quinoline does not occur directly because of the greater strength of the C–N bonds and is a complex sequential reaction involving hydrogenation of the N-ring, hydrogenolysis of the aliphatic C–N bond (CNH), hydrogenation of the C6-ring (HYD), and elimination of ammonia. A simplified sequence of steps is shown in Scheme 1.

On sulfides detailed kinetic studies show that the rates of HYD and CNH are of a similar order of magnitude, and no single rate-limiting step is operative [37,38]. On phosphides such studies have not been carried out, but it is likely that again no single rate-limiting step is involved and that CNH will be one of the key steps. This bond scission is difficult because of the steric constraints of the ring. The CNH reaction is a complex reaction and requires multiple sites [39–41], among them an acid site to bind the nitrogen compound and a proximal basic site to carry out a β -H attack. Thus, the reaction is structure-sensitive. Changes of P levels on the surface may disrupt the dual site and cause the observed maximum in activity with P content. The phosphidic P^{3-} may act as a base, in a manner similar



Scheme 1. Sequence of steps in quinoline hydrodenitrogenation.

to sulfidic S^{2-} , and assist in abstracting a proton from the adsorbed nitrogen-ring intermediate.

A concern with the use of any catalyst is its stability in the reaction medium. Mo, W, and Ni phosphides were tested for 100 h and did not display deactivation [13,36]. Analysis of the products by XRD after reaction revealed that there was no change in bulk crystal structure. EXAFS analysis of the Ni_2P catalyst provides additional insight [36]. Fig. 9 compares the EXAFS spectra of the fresh (solid lines) and spent (dashed lines) samples with initial Ni/P ratios of 2/1, 1/2, and 1/3. The sample with initial Ni/P = 2/1 (Fig. 6a) shows a main peak with a shoulder at lower interatomic distance. In contrast, the samples with initial Ni/P = 1/2 and 1/3 (Figs. 9b, 9c) display two distinct peaks, whose lengths match those of Ni–Ni and Ni–P distances in Ni_2P . There is no resemblance to the features of NiO, Ni(OH)₂, or Ni metal. The sample with initial Ni/P ratio of 2/1 (Fig. 9a) has a Ni–Ni distance close to that of metallic Ni, and the amount of Ni_2P phase is smaller, as could be expected from the spreading of the metal and phosphorus components on the surface of the support. The lack of Ni_2P also explains its low activity. With the Ni_2P/SiO_2 sample with the excess phosphorus

(initial Ni/P = 1/3), the FT peak positions duly correspond to those of bulk Ni_2P , but the relative intensity of the Ni–P is enhanced. The extra phosphorus probably resides on the surface of the highly dispersed particles, breaking up the catalytically active ensembles and again reducing activity.

In all cases changes can be discerned in the catalysts after reaction (Figs. 9d–9f). The main Ni–Ni and Ni–P peaks are attenuated and a feature in between the peaks grows. Comparisons with bulk sulfide samples indicates the appearance of a Ni–S signal. Thus, the active surface is probably a phosphosulfide.

The finding that sulfur was present on the surface of the phosphide catalysts after reaction raises questions about the true nature of the catalysts. The most significant is whether the catalysts are actually sulfides supported on phosphides, and therefore not really a new composition. In order to answer this question, reactivity studies were undertaken to compare the mechanism of reaction on the phosphides to that on the sulfides. Concentration was placed on HDN, as it is more difficult than HDS, and as a demanding reaction is a good probe of the details of surface structure and composition.

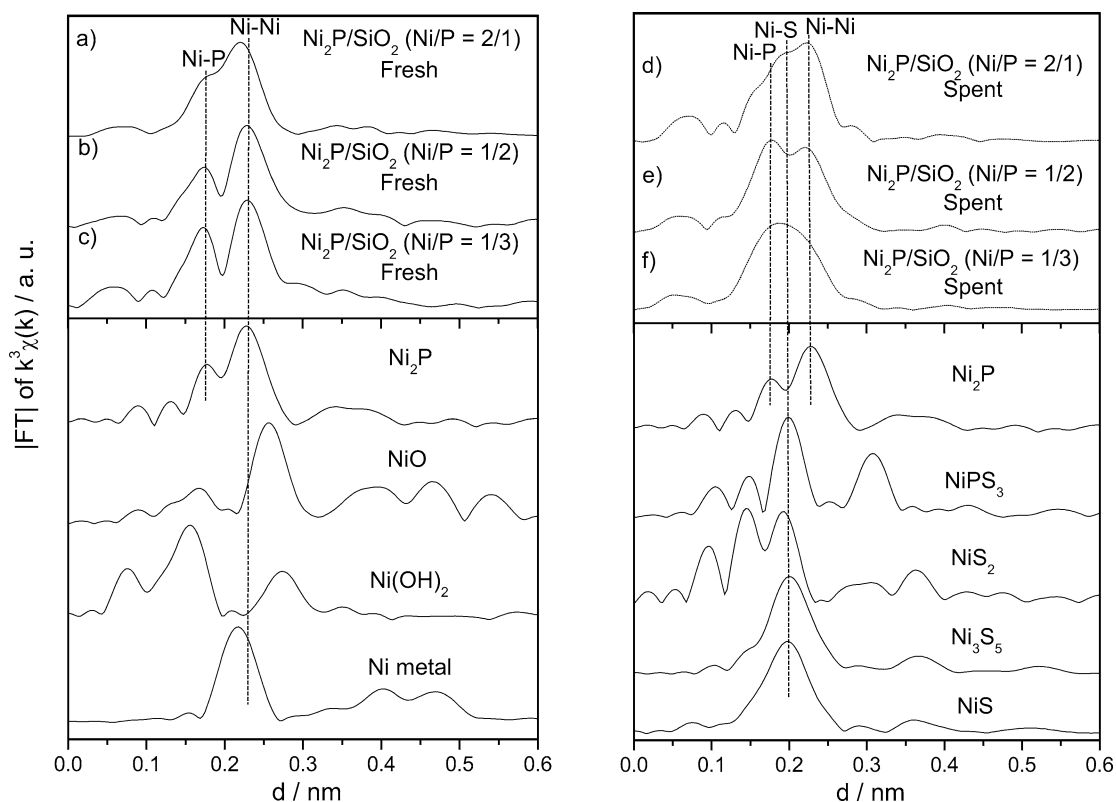


Fig. 9. EXAFS of the Ni_2P/SiO_2 catalyst (initial Ni/P = 1/2) before and after DBT reaction. (Reproduced from Ref. [36], with permission.)

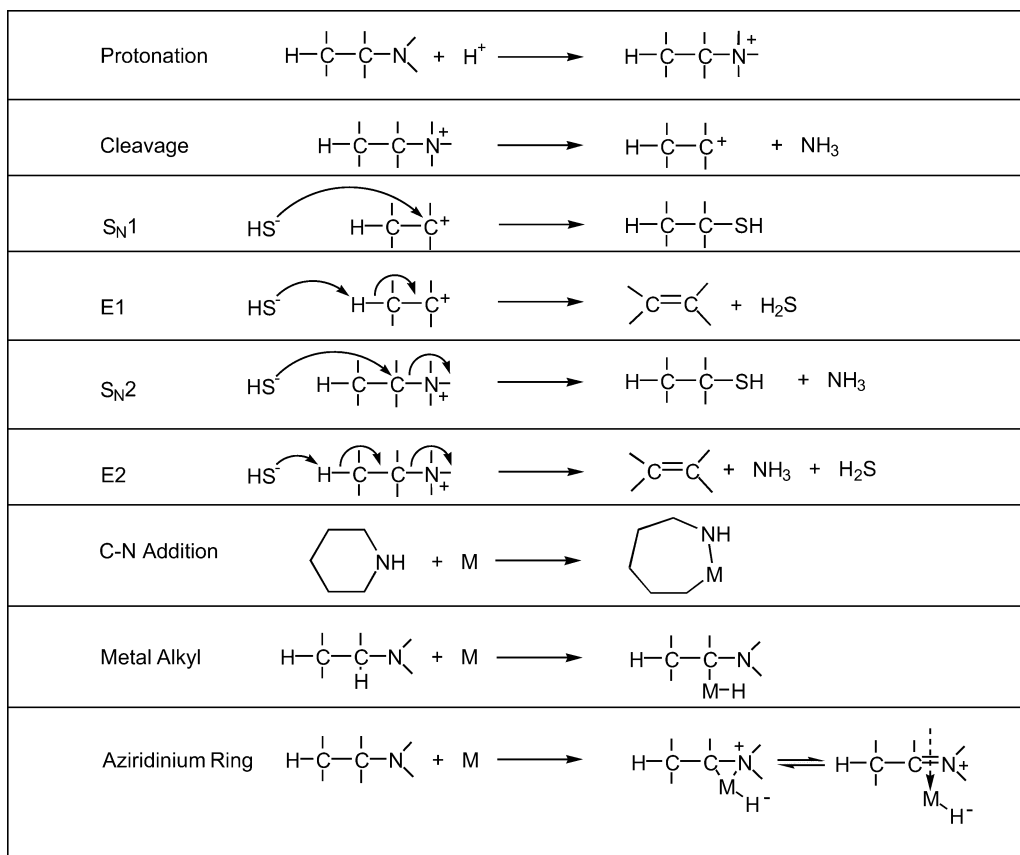


Fig. 10. Mechanisms and intermediates in C–N bond cleavage. (Reproduced from Ref. [42], with permission.)

6. Mechanism in HDN

A summary of possible reaction steps in HDN is presented in Fig. 10. These were described in detail in a previous publication [42], and only a brief summary will be presented here. The classical nitrogen removal mechanisms are nucleophilic substitution (S_N1, S_N2) or elimination (E1, E2). The mononuclear pathways (S_N1 and E1) start with the generation of a carbocation by quaternization of an amine followed by cleavage of ammonia, while the binuclear pathways (S_N2 and E2) proceed without scission of ammonia. The pathways involving reactions with metals (C–N oxidative addition and metal alkyl formation) require activation of the α -carbon to the nitrogen [43–45]. These last studies have been carried out with well-defined organometallic complexes, which serve as excellent models of the chemistry on heterogeneous catalyst surfaces. The mechanism of HDN in the present study was probed by determining the effect of molecular structure on reactivity.

In a first study, the C–N bond-breaking step was examined using a series of homologous pentylamines (Table 4) [42], as also studied on sulfides [46]. This corresponds to the last step in Scheme 1. The original work was carried out in the vapor phase, but for the present studies more realistic conditions of liquid phase and high pressure (3.1 MPa) were used. Comparison was made to a simple sulfide deposited on a noninteracting support, MoS₂/SiO₂, in order to avoid complications due to promoters and acidity.

The reactivity order was found to be *t*-pentylamine > *n*-pentylamine > *neo*-pentylamine, and this correlated with the number of β -H atoms relative to the N atom (Table 4). The order could not be explained by the involvement of α -H atoms, or of carbenium or carbanions formed at the amine position, and eliminated S_N1, S_N2, and E1-type mechanisms. This made the likely mechanism an E2 process involving surface attack by a nucleophilic species on a β -H atom. The same mechanism was found for WP/SiO₂, MoP/SiO₂, and MoS₂/SiO₂.

Table 4
Reactivity pattern of pentylamines


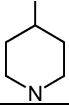
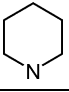
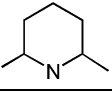
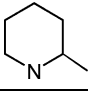
Reactivity		>		>	
Number of α -H's	0		2		2
Number of β -H's	8		2		0

Table 5
Reactivity pattern of piperidines

Reactivity		~		>		>	
Number of α -H's	4		4		2		3
Number of β -H's	4		4		10		7

In an ongoing study [47], the ring-opening step in N-heterocycles was probed on Ni₂P/SiO₂ using a family of piperidine derivatives (Table 5). This addresses the second step in Scheme 1, which is also a C–N bond-breaking reaction. A similar comparison was carried out on a commercial Ni–Mo–S/Al₂O₃ [48], and it was concluded that again a β -elimination was operative. In the case of the Ni₂P catalyst the results were not consistent with this. Here, it was found that the less hindered piperidines were more reactive than the more substituted piperidines, even though the latter had larger numbers of β -H atoms. The complete results will be discussed in a forthcoming paper [47], but it was found that the reactivity order was also not related to the formation of carbenium or carbanions. The most likely single reaction pathway is initial activation of the heterocycle at an α position, as shown in the bottom three entries of Fig. 10. Once activated, the N-containing ring can undergo further reaction by mechanisms involving elimination of β -H's. The preliminary conclusion is that the manner of N-removal is different on phosphides and sulfides, and this may account for the enhanced activity found on the phosphides.

7. Conclusions and perspective

The transition metal phosphides are an interesting class of compounds that combine the physical properties of ceramic compounds, such as hardness and strength, with the transport properties of metals, such as thermal and electrical conductivity. They can be prepared readily from inexpensive phosphate precursors by reduction in hydrogen. They show remarkable catalytic properties, in particular for HDS and HDN, with superior performance on a site and weight basis over commercial sulfide catalysts. Yet their general catalytic behavior has not been explored, and this remains an area of substantial promise. They should probably have good activity in hydrogen transfer reactions, such as hydrogenation, Fischer–Tropsch and ammonia synthesis, NO reduction, and electrochemical reductions. Of particular promise is the possibility of making multicomponent alloys.

Acknowledgments

Support for this work came from the US Department of Energy, Office of Basic Energy Sciences, through Grant DE-FG02-963414669, the NEDO International Joint Research Program, the LNLS (National Synchrotron Light

Laboratory) in Campinas, Brazil, under Project XAS 592/99, the Tsukuba Photon Factory of the High Energy Accelerator Research Organization under Grant 2001G297, and Brookhaven National Laboratory under Grant 4513. Individuals who were involved in the work were W. Li, P. Clark, X. Wang, Y.-K. Lee, P. Deck, F. G. Requejo, J.M. Ramallo-López, S. Hayashi, T. Sato, and Y. Yoshimura. M.E. Bussell kindly provided the TEM micrographs. The Journal of Catalysis gave permission to reproduce past work.

References

- [1] M.E. Davis, *Nature* 417 (2002) 813.
- [2] A. König, G. Herding, B. Hupfeld, Th. Richter, K. Weidmann, *Top. Catal.* 16/17 (2001) 23.
- [3] P. Greening, *Top. Catal.* 16/17 (2001) 5.
- [4] B.I. Bertelsen, *Top. Catal.* 16/17 (2001) 15.
- [5] K.G. Knudsen, B.H. Cooper, H. Topsøe, *Appl. Catal. A Gen.* 189 (1999) 205.
- [6] S.T. Oyama, C.C. Yu, S. Ramanathan, *J. Catal.* 184 (1999) 535.
- [7] C.C. Yu, R. Ramanathan, S.T. Oyama, *J. Catal.* 173 (1998) 1.
- [8] C. Song, A.D. Schmitz, *Energy Fuels* 11 (1997) 656.
- [9] Y. Yoshimura, H. Yasuda, T. Sato, N. Kijima, T. Kameoka, *Appl. Catal. A Gen.* 207 (2001) 303.
- [10] W. Li, B. Dhandapani, S.T. Oyama, *Chem. Lett.* (1998) 207.
- [11] C. Stinner, R. Prins, T. Weber, *J. Catal.* 191 (2000) 438.
- [12] C. Stinner, R. Prins, Th. Weber, *J. Catal.* 202 (2001) 187.
- [13] D.C. Phillips, S.J. Sawhill, R. Self, M.E. Bussell, *J. Catal.* 207 (2002) 266.
- [14] P. Clark, X. Wang, S.T. Oyama, *J. Catal.* 207 (2002) 256.
- [15] P. Clark, W. Li, S.T. Oyama, *J. Catal.* 200 (2001) 140.
- [16] S.T. Oyama, P. Clark, X. Wang, T. Shido, Y. Iwasawa, S. Hayashi, J.M. Ramallo-López, F.G. Requejo, *J. Phys. Chem. B* 106 (2002) 1913.
- [17] W.R.A.M. Robinson, J.N.M. van Gastel, T.I. Korányi, S. Eijssbouts, J.A.R. van Veen, V.H.J. de Beer, *J. Catal.* 161 (1996) 539.
- [18] X. Wang, P. Clark, S.T. Oyama, *J. Catal.* 208 (2002) 321.
- [19] T.I. Korányi, *Appl. Catal. A Gen.* 237 (2002) 1.
- [20] F. van Looij, P. van der Laan, W.H.J. Stork, D.J. DiCamillo, J. Swain, *Appl. Catal. A Gen.* 170 (1998) 1.
- [21] B. Aronsson, T. Lundström, S. Rundqvist, *Borides, Silicides and Phosphides*, Methuen, London/Wiley, New York, 1965.
- [22] D.E.C. Corbridge, *Studies in Inorganic Chemistry*, fourth ed., Vol. 10, Elsevier, Amsterdam, 1990.
- [23] G.Z. Hägg, *Phys. Chem.* 12 (1931) 33.
- [24] S. Rundqvist, *Colloq. Int. Cent. Nat. Rech. Sci.* 157 (1967) 85.
- [25] C. Stinner, Z. Tang, M. Haouas, Th. Weber, R. Prins, *J. Catal.* 208 (2002) 456.
- [26] E.L. Muetterties, J.C. Sauer, *J. Am. Chem. Soc.* 96 (1974) 3410.
- [27] F. Nozaki, M. Tokumi, *J. Catal.* 79 (1983) 207.
- [28] T. Nozaki, F. Kitoh, T. Sodesawa, *J. Catal.* 62 (1980) 286.
- [29] H. Li, W.-L. Dai, W. Wang, Z. Fang, J.-G. Deng, *Appl. Surf. Sci.* 152 (1999) 25.
- [30] S.-H. Ko, T.-C. Chou, *Can. J. Chem. Eng.* 72 (1994) 862.

- [31] W.-J. Wang, M.-H. Qiao, H. Li, J.-F. Deng, *Appl. Catal. A* 166 (1988) L243.
- [32] H. Li, W. Wang, B. Zong, E. Min, J.-F. Deng, *Chem. Lett.* (1998) 371.
- [33] J. Shen, B.E. Spiewak, J.A. Dumesic, *Langmuir* 13 (1997) 2735.
- [34] S.T. Oyama, X. Wang, F.G. Requejo, T. Sato, Y. Yoshimura, *J. Catal.* 209 (2002) 1.
- [35] J.T. Miller, W.J. Reagan, J.A. Kaduk, C.L. Marshall, A.J. Kropf, *J. Catal.* 193 (2000) 123.
- [36] S.T. Oyama, X. Wang, K.Y.-K. Lee Bando, F.G. Requejo, *J. Catal.* 210 (2002) 207.
- [37] B.K. Hodnett, B. Delmon, *Stud. Surf. Sci. Catal.* 27 (1986) 53.
- [38] I.A. van Parijs, G.F. Froment, B. Delmon, *Bull. Soc. Chim. Belg.* 93 (1984) 823.
- [39] J.A. Marzari, S. Rajagopal, R. Miranda, *J. Catal.* 156 (1995) 255.
- [40] M. Jian, R. Prins, *J. Catal.* 179 (1998) 18.
- [41] F. Rota, V.S. Ranade, R. Prins, *J. Catal.* 200 (2001) 389.
- [42] P. Clark, X. Wang, P. Deck, S.T. Oyama, *J. Catal.* 210 (2002) 116.
- [43] R.M. Laine, *Cat. Rev.-Sci. Eng.* 25 (1983) 459.
- [44] M.H. Chisholm, *Polyhedr.* 16 (1997) 3071.
- [45] K.J. Weller, P.A. Fox, S.D. Gray, D.E. Wigley, *Polyhedr.* 16 (1997) 3139.
- [46] M. Cattenot, J.L. Portefaix, J. Afonso, M. Breyse, M. Lacroix, G. Perot, *J. Catal.* 173 (1998) 366.
- [47] S.T. Oyama, X. Wang, in preparation.
- [48] J.L. Portefaix, M. Cattenot, M. Gueriche, J. Thivolle-Cazat, M. Breyse, *Catal. Today* 10 (1991) 473.